2019 EAGE ANNUAL
81ST CONFERENCE + EXHIBITION
LONDON | THE UNITED KINGDOM

We_R08_05

High-Resolution Velocity Model Building and Imaging for Injectites in the Central North Sea

S. Bretherton[1]*, R. Haacke[1], B. Xiao[1], M. Sinha[1], P. Roy[1], M. Ackers[2], C. Ward[2], A. Fletcher[2], D. Danchenko[2]

[1] CGG; [2] Spirit Energy

Summary

The central North Sea presents a number of difficulties for velocity model building and seismic imaging. In relatively shallow waters, acquisition geometries typically used for 3D seismic exploration leave little scope for reflection tomography to update the near surface velocity. Shallow gas pockets complicate both velocity estimation and imaging at depth, and anisotropy is difficult to estimate or validate without near-surface well control. Under these conditions Full Waveform Inversion (FWI) provides an option for velocity estimation. We present a 3-parameter workflow addressing velocity, absorption factor (Q), and epsilon. This is achieved with double application of 2-parameter joint FWI, solving first for Vp/Q then Vp/epsilon. This improves the imaging and positioning of complex injectite structures around 2.1 km depth. Beyond the needs of seismic imaging, we also seek an increased level of detail in the final velocity model for use as the low-frequency contribution to impedance inversion. This is achieved by altering the FWI to balance the contributions of reflections and refractions to the global gradient and cost function. By carefully increasing the weight of reflections, the level of velocity detail is increased at injectite level whilst maintaining the stability of the inversion and velocity estimate brought by refractions.

Introduction

Seismic exploration data in the central North Sea is typically acquired with 50-100 m cable separation and the nearest receivers offset by 100 m or more from the source. Consequently, due to missing near-angle information from near surface reflectors, high-resolution velocity model building and imaging can prove challenging. Recent progress in this area (McLeman et al., 2018) relies on Full Waveform Inversion (FWI) to make an accurate estimation of near-surface velocity (Vp). By incorporating a dispersive absorption factor (Q) to the velocity model, near-surface gas bodies can also be described well using 2-parameter Vp/Q joint FWI (Xiao et al., 2018). Nevertheless, high-resolution velocity-model building and imaging requires further efforts to estimate properties of the near-surface, notably the epsilon anisotropy parameter. This presents particular difficulties since borehole logs, from which an anisotropy estimate can be calibrated, are not typically recorded in the first few hundred metres below the waterbottom. An accurate epsilon model is required for FWI to recover an accurate Vp, and thus for the seismic image to be positioned correctly in depth. In addition to producing high fidelity images, an accurate and high-resolution velocity model provides geological detail for the low-frequency background functions used in acoustic impedance inversion (Jones et al., 2018). With complex geological structures present between the well locations, this approach is preferable to the use of well logs interpolated between sparse boreholes.

Sand injectites (Hurst and Cartwright, 2007) present local geological complexity that is challenging to capture between boreholes. Sand injectites are formed during burial, as overpressured sand bodies become remobilized and are forced upwards into sediment layers above. Injectite systems include complex geometries and small-scale steep dips with thin structures. Sand injectites can play an important role in the hydrocarbon system (Murphy and Wood, 2011), and are therefore targets for seismic impedance inversion.

This paper describes a workflow for high-resolution 3-parameter velocity estimation, addressing Vp, Q, and epsilon with two sequential passes of 2-parameter FWI. In addition, a method is described for re-balancing the contributions of reflections and refractions in FWI to increase the level of detail in the final Vp model while maintaining stability. This is applied to characterise a system of sand injectites at approximately 2.5 km depth in the central North Sea, with water depth around 160 m.

Method

Using a towed-streamer dataset acquired with 8 cables of 6 km length, a high-resolution velocity model was built using FWI to estimate Vp, Q and epsilon. The initial anisotropy model was adopted from a legacy model built mainly with reflection tomography (Guillaume et al., 2013), and assuming vertical transverse isotropy. With no sonic log data available in the uppermost 500 m, guided wave inversion (Hou et al., 2018) was used to improve the initial Vp estimate at and just below the seabed. Beneath this, interpolation of band-limited sonic logs provided an initial Vp model good enough to commence FWI with a starting frequency of 6 Hz.

The seismic image produced with Kirchhoff pre-stack depth migration from the legacy velocity model showed the presence of localised gas pockets through the survey area at around 450 m depth. A 2-parameter Vp/Q joint FWI was used to model absorbing bodies following the workflow described by

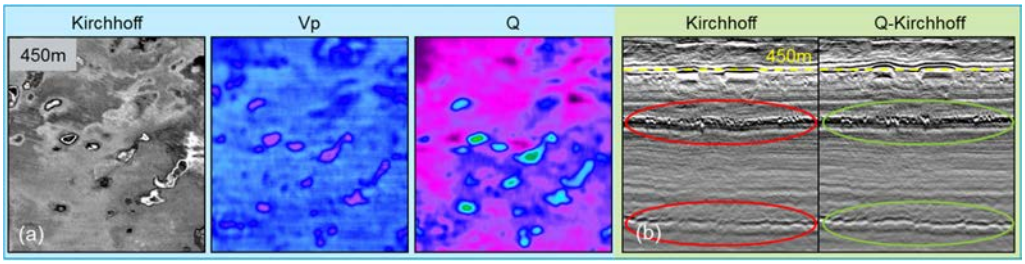

Figure 1. *(a) Depth slices through the results of Vp/Q joint FWI. (b) Comparison of Kirchhoff migration with legacy model vs Q-Kirchhoff migration with final FWI model.*

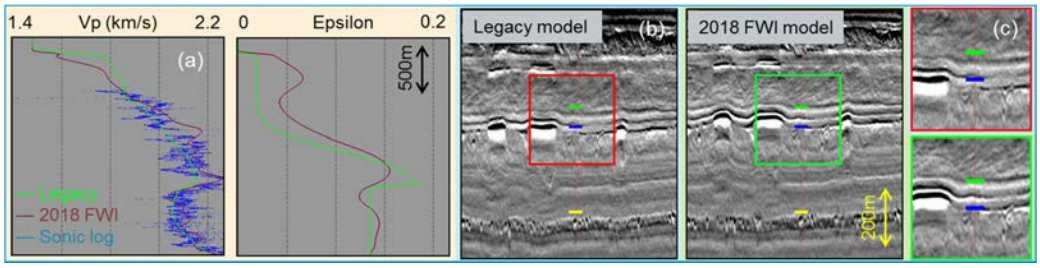

***Figure 2**. Comparison of legacy tomographic model and final 2018 FWI model (a), with corresponding Q-Kirchhoff migrated images (b). Annotated well-log formation tops highlight the depth improvement brought by the Vp/epsilon joint inversion (c).*

Xiao et al. (2018), based on earlier work by Malinowski et al. (2011) and Plessix et al. (2016). Cross-talk between Vp and Q was reduced by broadening the bandwidth of the joint FWI to a maximum frequency of 8 Hz, with no explicit low-frequency limitation. The final migration (Figure 1) shows improvement in focus and broad-band amplitude recovery below absorbing low-Q bodies.

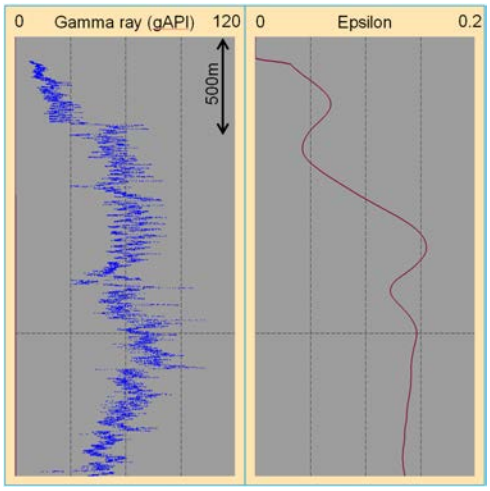

***Figure 3**. Gamma ray log vs updated epsilon*

The updated Q model was then used to initiate a 2-parameter Vp/epsilon joint FWI with focus on the uppermost 500 m, in which the velocities were not constrained by well data. This time, cross-talk between Vp and epsilon was reduced by mixing refractions and reflections to ensure the illumination of the subsurface was sufficient for the inversion to detect the differences in radiation patterns of these two parameters. After running the joint FWI to 8 Hz, the epsilon model showed significant changes from the starting point (Figure 2), increasing from approximately 3 % in the near surface to approximately 7 % in a discrete near-surface layer. The Vp model responded accordingly, with lower near-surface values and larger velocity gradient. This time, migration tests showed significant improvement of the depth tie between seismic markers around 500 m depth and corresponding lithological tops identified in boreholes (Figure 2). This was achieved without explicit depth calibration of the velocity model. Notably, gamma-ray logs qualitatively indicate changes in lithology that coincide with discrete macro-layers starting to appear in the updated epsilon model (Figure 3). In the deeper parts of the model, epsilon remained close to the trend of the legacy model.

The final phase of the model update was a high-frequency pass of FWI with focus on adding detail to the Vp parameter. Using diving waves in FWI run to 15 Hz, it was seen that the near-surface was updated with an adequate level of detail, and that the model was improved at injectite depth but without the required level of detail. These tests were repeated with an open mute to incorporate reflections into the FWI gradient and cost function. However, this was not effective as the locally hard waterbottom generates strong guided waves and diving waves which dominate the inversion (Figure 4), overwhelming the contribution made from relatively weak and chaotic reflections. For interest, the FWI was then repeated with reflections only (i.e. guided waves and diving waves muted from the data and the residuals). The result showed increased detail at injectite depths, but there was strong near-surface acquisition footprint in the FWI gradient. In addition it was unclear how the effect of density changes in the subsurface would affect an FWI update based only on reflections. The third approach was thus to separate the refractions (which bring stability and reduce the influence of density changes on the velocity update) and reflections (which add detail at injectite depth) and to incorporate both to the FWI with a weighting scheme designed to balance their contributions to the gradient and cost function. The weighting was applied to residuals before back propagation. To avoid over-scaling the

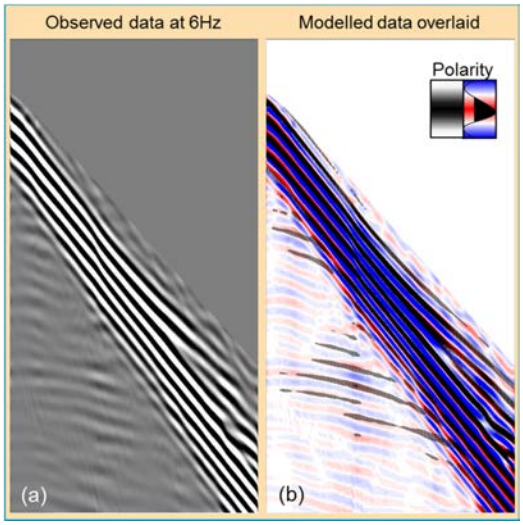

Figure 4. *Observed data at 6 Hz (a) shows low amplitude reflections compared with diving waves and guided waves. 5 second record length showing full 6 km offset with model shot after FWI (b).*

contribution to the cost function, the dot product of residuals was normalised again by the weight for each shot. In response to the separation and re-weighting of reflections and refractions, the FWI was able to maintain stability in the near surface while adding plausible detail at injectite depth (Figure 5). The contribution of diving waves at injectite depths should help mitigate the effect of density errors in the velocity update, but this cannot easily be shown except by comparing the result of seismic impedance inversion to blind well logs.

Results

The improvement in image depth accuracy after the Vp/epsilon joint FWI indicates a good overall recovery of the average velocity in the uppermost parts of the model. Meanwhile, the development of discrete low-Q gas bodies helps reduce localised distortion of the image and compensate for the attenuation of higher frequencies after Q-Kirchhoff depth migration. The final higher-frequency pass of Vp-only FWI produces the level of detail required for use as the background impedance trend between boreholes. This step was much improved by separating the reflections and refractions then re-combining with different weights to better balance their contributions to the FWI. The improvement in the final FWI model, compared with the legacy model, is significant (Figure 6). The improvement is expressed through better imaging and reflector positioning in depth, relative to well data, in addition to an improved low-frequency contribution to impedance inversion.

Conclusions

This workflow, employing Vp/Q and Vp/epsilon joint FWI followed by a Vp update using re-weighted diving wave and reflection data, helps produce a high-resolution velocity model with improved accuracy of image depth and fidelity under local gas bodies. By splitting reflections and refractions then re-combining them in FWI with different weighting, it was possible to tune the level of detail recovered deeper in the model, with potential velocity errors related to density changes

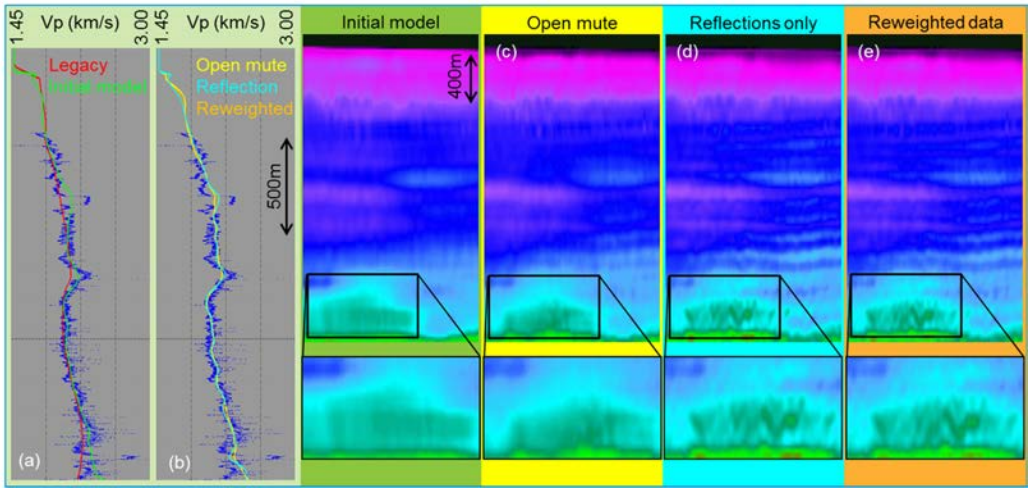

Figure 5 *Comparison of starting (a) and final (b) FWI velocity models, highlighting differences in injectite bodies recovered by FWI with no mute (c), reflections only (d), and re-weighted reflection and refraction data (e).*

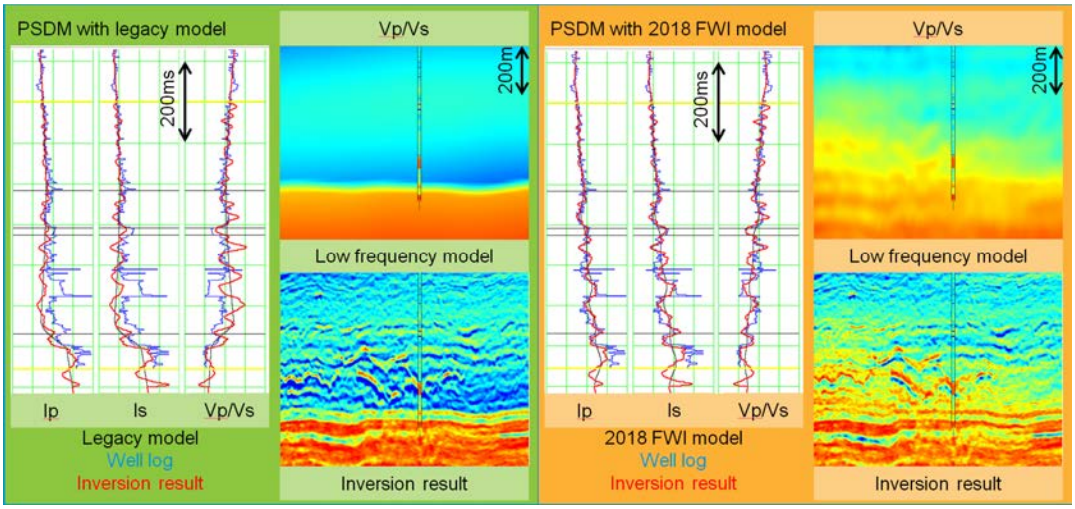

***Figure 6**. Inversion results from PSDM of the legacy and 2018 FWI models.*

mitigated by the balanced inclusion of diving waves. In a 3-parameter model build, there is concern of cross-talk between velocity, Q, epsilon and density. Accurate reflector depthing and reduction of push-down below gas bodies in the final depth image are signs that this is mitigated with respect to epsilon and Q. Residual cross-talk errors related to density changes remain, but re-balancing the contributions of reflections and diving waves helps reduce this where both wave types have appreciable illumination. For our example with sand injectites in the central North Sea, this method has produced a velocity model with direct application as a low-frequency impedance contribution.

Acknowledgements

We would like to thank CGG Multi-Client & New Ventures for permission to publish.

References

Guillaume, P., Montel, J. P., Hollingworth, S., Zhang, X., Prescott, A., Reinier, M., Jupp, R., Lambare, G., Pape, O. and Cacalie, A. [2012] Seismic imaging with multi-layer tomography. *First Break*, **30**, 85-90.

Hou, S., Haacke, R. R., Corbett, A. and Wanczuk, M. [2018] Velocity Model Building with Guided Wave Inversion. *80th EAGE Conference & Exhibition*, 10.3997/2214-4609.201801164.

Hurst, A. and Cartwright, J. [2007] Sand injectites: Implications for hydrocarbon exploration and production. *AAPG Memoir*, **87**.

Jones, I. F., Singh, J., Greenwood, S., Chigbo, J., Cox, P. and Hawke, C. [2018] High-resolution impedance estimation using refraction and reflection FWI constraints: the Fortuna region, offshore Equatorial Guinea. *First Break*, **11**, 39-44.

Malinowski, M., Operto, S., and Ribodetti, A. [2011] High-resolution seismic attenuation imaging from wide-aperture onshore data by visco-acoustic frequency-domain full-waveform inversion. *Geophysical Journal International*, **186**, 1179-1204.

McLeman, J., Xiao, B., Page, C., Jouno, F., Salaun, N., Roubaud, A. and Perrone, F. [2018] Next Generation Shallow Water Resolution: Primary Wave Imaging and High Frequency Visco-acoustic Full-waveform Inversion. *80th EAGE Conference and Exhibition*, 10.3997/2214-4609.201801163.

Murphy, S.D. and Wood, P.H. [2011] Palaeogene remobilized sandstones of the Central North Sea – implications for hydrocarbon migration. *First Break*, **29**, 45-55.

Plessix, R. E., Stopin, A., Kuehl, H., Goh, V. and Overgaag, K. [2016] Visco-acoustic full waveform inversion. *78th EAGE Conference and Exhibition*, 10.3997/2214-4609.201600827.

Xiao, B., Ratcliffe, A., Latter, T., Xie, Y. and Wang, M. [2018] Inverting for near-surface absorption with full-waveform inversion: a case study from the North Viking Graben in the northern North Sea. *80th EAGE Conference and Exhibition*, 10.3997/2214-4609.201800681.